

1 **Construction of whole cell bacterial biosensors as an alternative environmental
2 monitoring technology to detect naphthenic acids in oil sands process-affected
3 water.**

4

5 Tyson Bookout^b, Steve Shideler^b, Evan Cooper^{a,b}, Kira Goff^{a,b}, John V Headley^c, Lisa M
6 Gieg^d, and **Shawn Lewenza**^{a,b*}

7

8 ^a Faculty of Science and Technology, Athabasca University, Athabasca, Alberta, Canada

9 ^b-Department of Microbiology, Immunology and Infectious Diseases, University of
10 Calgary, Calgary, Alberta, Canada

11 ^c Environment and Climate Change Canada, National Hydrology Research Centre,
12 Saskatoon, Saskatchewan, Canada

13 ^d Biological Sciences, University of Calgary, Calgary, Alberta, Canada

14

15 * slewenza@athabascau.ca Corresponding Author

16

17 Running title: Biosensors for specific naphthenic acid detection in water

18

19

20

21

22 **Abstract**

23 After extraction of bitumen from oil sands deposits, the oil sand process-affected water
24 (OSPW) is stored in tailings ponds. Naphthenic acids in tailings ponds have been
25 identified as the primary contributor to toxicity to aquatic life. As an alternative to other
26 analytical methods, here we identify bacterial genes induced after growth in naphthenic
27 acids and use synthetic biology approaches to construct a panel of candidate biosensors
28 for NA detection in water. The main promoters of interest were the *atuAR* promoters from
29 a naphthenic acid degradation operon and upstream TetR regulator, the *marR* operon
30 which includes a MarR regulator and downstream naphthenic acid resistance genes, and
31 a hypothetical gene with a possible role in fatty acid biology. Promoters were printed and
32 cloned as transcriptional *lux* reporter plasmids that were introduced into a tailings pond-
33 derived *Pseudomonas* species. All candidate biosensor strains were tested for
34 transcriptional responses to naphthenic acid mixtures and individual compounds. The
35 three priority promoters respond in a dose-dependent manner, which allows semi-
36 quantitative measurements, to simple, acyclic and complex NA mixtures, and each
37 promoter has unique NA specificities. The limits of NA detection from the various NA
38 mixtures ranged between 1.5 - 15 mg/L. The *atuA* and *marR* promoters also detected NA
39 in small volumes of OSPW samples and were induced by extracts of the panel of OSPW
40 samples. While biosensors have been constructed for other hydrocarbons, here we
41 describe a biosensor approach that could be employed in environmental monitoring of
42 naphthenic acids in oil sands mining wastewater.

43

44

45 **Introduction**

46 The Athabasca oil sands in northern Alberta represent one of the world's largest
47 sources of recoverable bitumen (1). Bitumen is a heavily biodegraded crude oil recovered
48 from surface mining the oil sands through the Clark process, or alkaline hot water
49 extraction (2, 3). After separation of the oil from the extraction water, the resulting oil
50 sands process-affected water (OSPW) is deposited and stored in tailings ponds where
51 solids can settle, and the water can be recycled for repeat extractions (1). In addition to
52 sand, silt, and clay, the OSPW contains many compounds such as dissolved ions, heavy
53 metals, unrecovered oil, and numerous acid-extractable organic (AEO) compounds like
54 naphthenic acids (1-3).

55 Naphthenic acids (NA) are naturally produced during the degradation of petroleum
56 and are present in the oil sands ore used to produce bitumen. Naphthenic acid
57 concentrations at the low end (5-30 mg/L) are in-line with concentrations observed in
58 Athabasca wetlands (4), and mid-range concentrations (50 – 120 mg/L) are in-line with
59 OSPW and industrially-affected experimental wetlands (3, 2, 5, 6). They are classically
60 defined by the formula $C_nH_{2n-z}O_2$, where n is the number of carbons and Z indicates the
61 number of hydrogens lost due to ring formation, and comprise a complex mixture of
62 monocyclic, polycyclic, and acyclic alkyl-substituted carboxylic acids (2). The NAFCs
63 extracted from OSPW have been characterized at the molecular level by Headley et al.
64 and others according to distribution of classical NA based on carbon number; double bond
65 equivalence and number of rings; along with heteroatomic (e,g S, N) content (7, 4, 6).
66 NA have been identified as the main contributor to OSPW toxicity, and have
67 demonstrated toxicity in microbes, plants, fish, amphibians, birds and mammals (3, 5, 8).

68 Some naphthenic acid compounds are difficult for bacteria to degrade, particularly those
69 high molecular weight compounds containing multi-ringed structures and branched
70 carboxylic acids (3).

71 Standard practice in the oil sands industry is to store OSPW in large tailings ponds.
72 Despite OSPW recycling, this has resulted in the accumulation of over 1 billion m³ of
73 OSPW (9). There are currently no established, cost-effective methods available to
74 remediate the organic contaminants in the tailings ponds on the large scale required, prior
75 to eventual discharge back to the natural environment. There are various analytical
76 methods for monitoring and quantifying NA, including conventional screening techniques
77 such as Gas Chromatography-Mass Spectrometry (GC-MS), Fourier Transform Infrared
78 Spectroscopy (FTIR), along with molecular level high resolution mass spectrometry
79 employing for example Fourier transform Ion cyclotron resonance or Orbitrap analysis
80 with Negative Ion Electrospray Ionization-Mass Spectrometry (ESI-MS), with or without
81 on-line High-Performance Liquid Chromatography (HPLC) (8, 10). These approaches are
82 semi-quantitative with relatively low limits of detection, as low as 0.01 mg/L with ESI-MS
83 (8). In general, the chemical analysis methods require multiple sample processing steps,
84 including an organic solvent extraction of OSPW, which may bias the analysis, and can
85 be time-consuming and costly (10). Hence, there is an opportunity for a rapid, cost-
86 effective method for sensitive NA detection and quantification.

87 Whole cell biosensors are engineered bacterial strains capable of detecting and
88 quantifying various compounds and analytes by producing a simple optical or
89 electrochemical output proportional to the analyte of interest (11). This proven technology
90 utilizes the refined metabolite sensing mechanisms of bacterial cells for detecting and

91 adjusting to changes in the surrounding environment, providing a particularly useful tool
92 for environmental monitoring. This technology is specific and capable of detecting low
93 levels of small molecules, including aromatic compounds, alkanes, alkenes, heavy
94 metals, and antibiotics (12–15). The sensitivity for biosensors are commonly in the parts
95 per million range (mg/L), though there have been some reporting in the range of parts per
96 billion (µg/L) (13, 16).

97 Bacterial biosensors are constructed by cloning a target analyte-induced promoter
98 as a transcriptional fusion to a reporter gene (*lacZ*, *gfp*, *luxCDABE*), which allows for a
99 simple, measurable output in response to exposure to the analyte in question. Using a
100 *Pseudomonas* species OST1909 derived from a tailings pond (17), we performed RNA-
101 seq to identify bacterial genes that are induced in response to various mixtures of
102 naphthenic acids. We then printed a large collection of promoters and constructed a panel
103 of transcriptional *luxCDABE* (bioluminescence) reporters to identify promoters that
104 uniquely respond to acyclic naphthenic acids, a simple naphthenic acids mix, and the
105 complex mixture of naphthenic acids that are extracted from OSPW, and untreated
106 OSPW directly. NA-inducible promoters were configured in various biosensor designs,
107 which were tested for their sensitivity and specificity of NA detection.

108

109 **Materials and Methods**

110 **Library construction, SOLiD sequencing and RNA-Seq analysis.**

111 For RNA isolation, *Pseudomonas* sp. OST1909 (15) was grown (~25°C) in TB medium
112 with 2% DMSO with or without 150 mg/L acyclic naphthenic acids (Sigma Aldrich

113 70340,15), or 150 mg/L of custom mix of 9X naphthenic acids (Table S1), or 150 mg/L
114 of acid extracted organics; namely naphthenic acid fraction compounds (NAFC) extracted
115 from oilsands process-affected water, which were prepared as previously described and
116 provided by Environment and Climate Change Canada (19). TB is buffered media (~pH
117 7) was used to prevent any pH change upon addition of NA. Total bacterial RNA was
118 isolated from duplicate, early-log cultures ($OD_{600} = 0.2$, 2×10^9 cells) using the Qiagen
119 RNeasy kit and stored in Qiagen RNA Protect. All subsequent steps were performed by
120 the Centre for Health Genomics and Informatics at the University of Calgary.

121 Total RNA samples were treated with DNase (Ambion) and assessed on an
122 Agilent 2200 TapeStation. Then ribosomal depletion (Ribo-Zero, Illumina) and
123 subsequent cDNA synthesis and conversion into sequencing libraries (SOLiD Total RNA-
124 Seq Kit, Life Technologies) was performed as per the kit protocols. The indexed libraries
125 were then pooled and added to SOLiD sequencing beads using emulsion PCR (EZ Bead
126 E80 kit, Life Technologies). The resulting beads were then applied to two lanes of a six
127 lane SOLiD 5500xl DNA sequencer for 75 bp sequencing. Each lane yield approximately
128 135 million reads (270M reads total). Transcriptome data has been assigned the GEO
129 accession number GSE262045.

130 Reads from the RNA-Seq experiment were mapped to the *Pseudomonas* sp.
131 OST1909 genome (17) using SHRiMP v2.2.3. (<http://compbio.cs.toronto.edu/shrimp/>; -v
132 50% -h 50%) (20). Samtools was then used to convert the .sam output into fasta format
133 (<http://www.htslib.org/>) for transcript analysis with Kallisto v0.46.1-0
134 (<https://pachterlab.github.io/kallisto/about>, downgraded to legacy version that outputs
135 bootstraps required by Sleuth) (21) and the sleuth package in R

136 (<https://pachterlab.github.io/sleuth/about>) (22). Kallisto quantified data by pseudo
137 alignment, assigning reads to reference transcripts based on kmer counts (-k=31 -b 100
138 -s 1). Transcript abundances and bootstraps were modeled in Sleuth and subjected to
139 statistical analysis via Wald test, modeled to remove transcripts occurring at low
140 abundances across all conditions. The Mann-Whitney *U* test was performed to measure
141 significant gene induction of all genes in an operon of interest.

142

143 **Construction of first, second and third-generation bioluminescent biosensors.** A
144 large panel of 54 promoters was targeted for DNA synthesis, combined with automated
145 Gibson assembly to clone as transcriptional *luxCDABE* reporters in the plasmid pMS402
146 (23) (**Table S2**). The BioXP 3200™ was used for synthesis of predicted bacterial
147 promoters, each with a minimum length of 165 bp that previously determined as a
148 functional length for thousands of synthetic promoters (24). However, if no BPROM (25)
149 predicted promoter was found within the first 165 bp upstream of the start codon, the
150 sequence length was extended to include the BPROM predicted promoter. The synthesis
151 was performed in a 96-well plate format which produced a recovery plate that contained
152 10 µl of transformation-ready ligated promoter *lux* constructs, in addition to 50 µl of each
153 synthesized promoter sequence. The pMS402 reporter plasmid is first linearized by
154 BamHI restriction digestion, and the promoter sequences are synthesized with an extra
155 30-40 bp on both 5' and 3' ends that are complimentary to the sequences flanking the
156 BamHI site. The linearized vector and synthesized promoter were mixed with the Gibson
157 assembly mix, which contains a 5' exonuclease, DNA polymerase, and ligase enzymes.
158 Except for linearizing the pMS402 vector, the cloning processes were conducted by

159 CODEX DNA's BioXP™ 3200. For the first generation of synthesis and cloning, we
160 maintained the pMS402 vector ribosome binding site (RBS) within 20 bp of the *luxC* start
161 codon. Therefore, these constructs contained the promoter and vector ribosome binding
162 sites (RBS) upstream of the *luxCDABE* operon. To optimize promoter cloning, we
163 removed the vector RBS during the Gibson assembly in the second-generation
164 constructs. The additional RBS between the promoter insertion site and the *lux* operon
165 was hypothesized to interfere with expression of the other promoters. All plasmids were
166 introduced into *Pseudomonas* OST1900 using electroporation.

167 A third-generation design was used in constructs with the *atuAR* and *marR*
168 promoters, where we also included the corresponding regulator gene *atuR* or *marR*,
169 respectively, upstream from the transcriptional reporter (Fig 1). The regulator gene was
170 driven low strength (data not shown), constitutive OST1909 promoter upstream of a
171 predicted BCCT family transporter (locus tag "IH404_RS26360"). To prevent gene
172 expression read through, strong terminators (26) were added downstream of the two
173 synthetic promoters (Table S2).

174

175 **Mini-Tn5-lux mutagenesis of *Pseudomonas* sp. OST1909 and screening for NA-
176 induced transcriptional fusions.** As previously described (27), random mini-Tn5-lux
177 mutagenesis was performed by mating the transposon from an *E. coli* donor into
178 OST1909, and selecting insertion mutants on LB + 50 µg/mL tetracycline. Colonies were
179 then stamped onto LB agar with and without 100 mg/ml of the custom mix of 9X
180 naphthenic acids, and were visualized using a chemiluminescence imaging system, to
181 identify colonies that had increased luminescence in the presence of NA. The genome of

182 one mutant of interest was sequenced using minION (Oxford Nanopore) in order to map
183 the *Tn* insertion site to the hypothetical gene with locus tag IH404_RS03680
184 (*hyp3680::lux*).

185

186 **High-throughput gene expression screening of biosensor constructs for specificity**
187 **and sensitivity to naphthenic acids.** Candidate biosensors were initially grown in tubes
188 at room temperature (~25°C) overnight in 3 mL LB media + 50 µg/mL kanamycin, to
189 maintain selective pressure on the promoter-*lux* plasmid and subcultured into M9
190 (Difco™, 248510) or BM2 (0.5 mM Mg²⁺) (28) minimal, defined media with 20 mM
191 succinate. The *lux* gene expression assays were conducted in black 96-well, clear bottom
192 plates (Thermo Scientific). NA were diluted to their final concentrations in 99 µl growth
193 media containing 2% DMSO to increase NA solubility, which was then inoculated with 1
194 µl of the overnight biosensor cultures. NA stock solutions were made according to **Table**
195 **S1.** Other hydrocarbons were tested to ensure the biosensor specificity for NA and certain
196 hydrophobic compounds such as alkanes and longer carbon chain carboxylic acids
197 required the solvent of 45% ethanol and 55% polyethylene glycol 400 (PEGEt) (29), at a
198 final concentration of 2%. A Breath-Easy® (Sigma-Aldrich) membrane was used to
199 prevent evaporation during a 15-hour protocol in a PerkinElmer 1420 multilabel counter
200 Victor³. The plate reader protocol (2 sec shake; gene expression in counts per second
201 (CPS), growth (OD₆₀₀)) included 45 time points, taken every 20 minutes. The gene
202 expression CPS value was typically normalized by dividing the CPS by the OD₆₀₀ for each
203 read. To compare the bioluminescent response of the different biosensor strains to the
204 various compounds tested, the Fold Gene Expression was also calculated by dividing the

205 CPS/OD₆₀₀ values of the NA treated sample by those of the untreated sample. A fold
206 change of 1 indicates no change, and a fold change of 2 indicates a doubling of *lux*
207 expression in comparison to the untreated control.

208

209 **Oil sands process water (OSPW) sample testing.** Water samples from the tailings
210 ponds in the mineable oil sands region, as well as naphthenic acid fraction components
211 (NAFC) extracted from the OSPW, were provided by Environment and Climate Change
212 Canada. Details are given elsewhere of the collection of OSPW; preparation of the NAFC
213 extracts, and molecular level analysis of NAFC by negative-ion electrospray ionization
214 high resolution Orbitrap mass spectrometry (4, 19). The concentrations of NAFC in both
215 the water samples and extracts were determined and recorded in **Table S1**. Depending on
216 the reported concentrations, the NAFC extracts were diluted by a factor of 10 or 100 and
217 tested at a final concentration between 20 and 60 mg/L. To monitor NA levels in the water
218 samples with minimal treatment or dilution, 90 μ l of each sample were added to each well of
219 the assay plate. This was supplemented with 10 μ l of 10x BM2 to allow for biosensor growth,
220 inoculated with 1 μ l biosensor culture, and measured as described above.

221

222 **Results and Discussion**

223 **Transcriptome analysis of genes induced during growth in the presence of**
224 **naphthenic acids.** In the presence of petroleum hydrocarbons, transcriptome studies
225 revealed that bacterial genes required to transport, metabolize or defend against these
226 environmental compounds are frequently induced (30–32). To identify genes regulated by

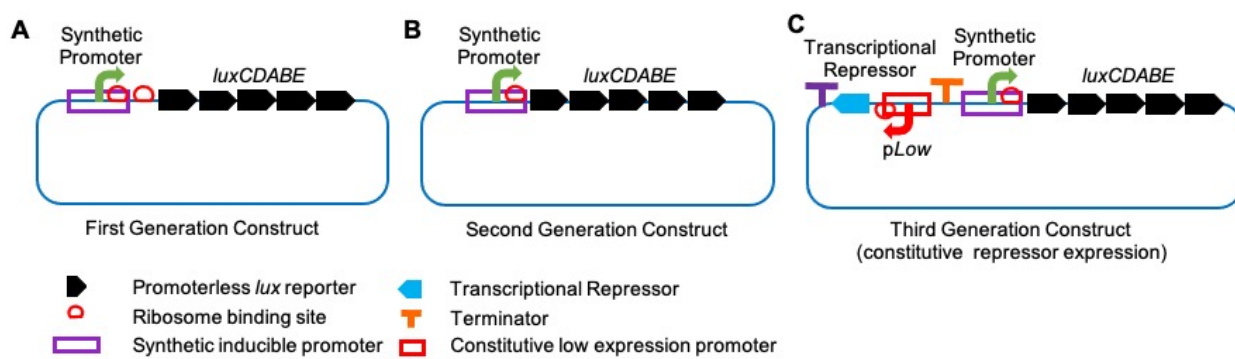
227 exposure to naphthenic acids, we performed RNA-seq experiments with *Pseudomonas*
228 *sp.* OST1909 (17) grown to mid-log phase in growth medium containing naphthenic acids.
229 To generate a diverse array of NA-induced genes, transcriptome experiments were
230 performed after adding 150 mg/L of three distinct naphthenic acid mixtures: acyclic
231 naphthenic acids (15) (Sigma-Aldrich, 70340), a custom mix of 9 individual naphthenic
232 acids (**Table S1**), or NAFC extracted from oilsands process-affected water (4, 19).

233 The upregulated genes included many genes annotated in metabolisms, fatty acid
234 degradation, nutrient transport in and out of the cell, and here we focussed on upregulated
235 metabolite sensing, transcriptional regulators (12) and their adjacent operons (**Table S3**).
236 RNA-seq showed significant upregulation of genes under experimental conditions:
237 OSPW (p<0.05 = 56; q<0.05 = 0; n=2), acyclic NA (p<0.05 = 140; q<0.05 = 18, n=2), and
238 9xNA (p<0.05 = 110; q<0.05 = 14, n=2). The genes induced by the custom 9xNA mix
239 involved in fatty acid degradation (β -oxidation) include the *fadAB* genes
240 (IH404_RS09140/5), *fadD1* (IH404_RS22010), *fadL* (IH404_RS20310) (33). The genes
241 induced by the acyclic NA mixture that encodes another possible NA degradation operon
242 is the IH404_RS15470-IH404_RS15515 cluster (**Table S3**). We prioritized 54 NA-
243 induced promoters for construction as plasmid-based transcriptional fusions, as
244 candidates for bacterial biosensors to be used to detect naphthenic acids (**Table S2**)
245 based on their upregulation in the transcriptome, and a predicted role in naphthenic acid
246 degradation, efflux, transport and small molecule sensing transcriptional repressors.

247

248 **Rapid construction of plasmid-encoded transcriptional fusions of NA-inducible**
249 **promoters controlling the *luxCDABE* transcriptional reporter genes.** Among the 54

250 promoters identified by RNA-seq, 26 promoters were induced in response to a
251 commercially available mixture of acyclic carboxylic acids, 14 promoters in response to
252 the simple mixture of nine NA compounds, 14 promoters in response to the naphthenic
253 acids that were acid extracted from OSPW (Table S2, S3). For large scale printing of
254 bacterial promoters, we used short upstream regions (165-350 bp) that contained
255 predicted sigma-70 promoter sequences (25) to drive the *luxCDABE* reporter. The first-
256 generation constructs included the ribosome binding site (RBS) within the promoter, in
257 addition to a second RBS present in pMS402 upstream of the *luxC* start codon. In the
258 second-generation constructs, we removed the vector-encoded RBS and included only
259 the RBS present in the predicted promoter region from *Pseudomonas* sp. 1909 (Fig 1).



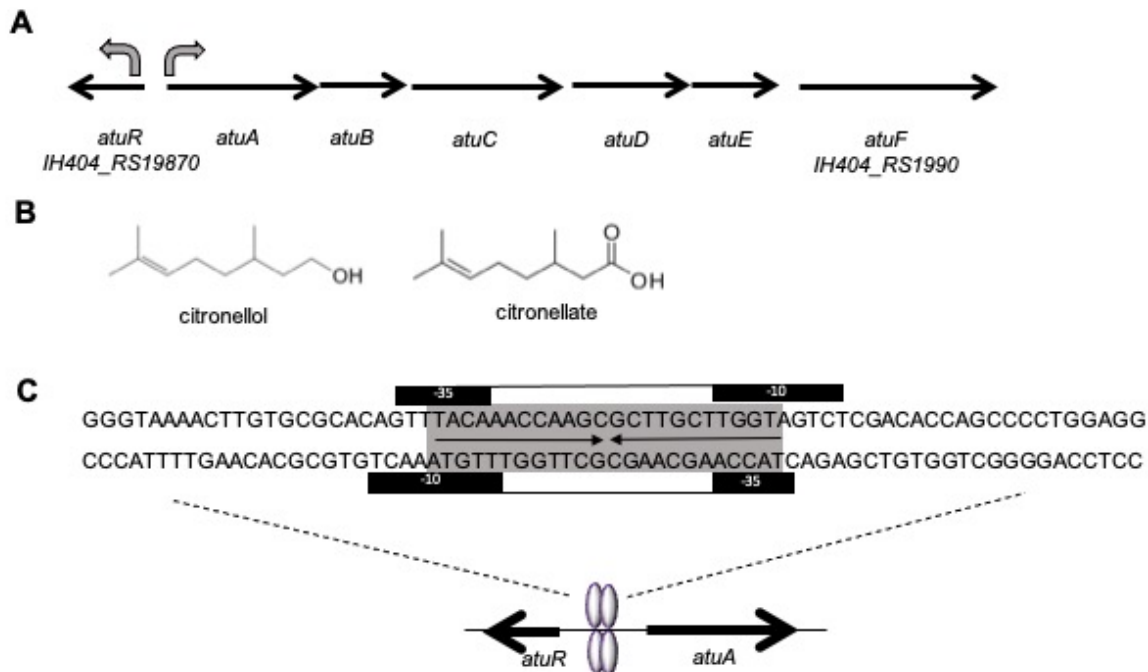
261 **Figure 1 – Genetic map of plasmid-based biosensor construct designs. A.** The
262 *luxCDABE* reporter genes (black) includes a RBS (red circle) upstream of the *luxC* start
263 site. The first generation constructs include the target promoter cloned as a transcriptional
264 *lux* fusion and includes a second RBS from the native promoter. **B.** The second
265 generation constructs have the plasmid RBS removed during Gibson assembly. **C.** Third
266 generation constructs also include the transcriptional repressor gene under the control of
267 a constitutive, low level expression promoter. Transcriptional terminators were added to
268 prevent any read through from upstream promoters.

269

270 **The *atuA* and *atuR* promoters from the *atu* operon are induced after detection of
271 acyclic naphthenic acids.** After a preliminary screen of all candidate biosensor strains,

272 we selected the mostly highly induced promoter from each of the three NA mixtures for
273 further study. In response to the acyclic NA mixture, we identified an operon that encodes
274 homologs of the *Pseudomonas aeruginosa* acyclic terpene utilization operon (*atu* operon)
275 (34–36) (**Fig 2, Table S3**). While individual genes within the cluster were induced, we
276 also confirmed induction of the whole *atu* operon using the *U* test ($p < 0.05$, **Table 1**). In *P.*
277 *aeruginosa*, terpenes and the carboxylic acids citronellate and geranylinate are degraded
278 by the *atu* genes, β -oxidation and the leucine-isovalerate utilization (*liu*) pathways (34–
279 36). Notably, the *P. aeruginosa* *atu* operon is induced in the presence of citronellate and
280 the acyclic monoterpenes citronellol and geraniol (34–36). The probable *Pseudomonas*
281 *sp.* OST1909 NA biodegradation cluster *atuA* through *atuF* (IH404_RS19870–
282 IH404_RS1990) is divergently expressed from the tetR-type transcription regulator AtuR
283 (IH404_RS19865) (37) (**Fig 2A**). Divergent promoters were detected in this intergenic
284 region (**Fig 2C**) and therefore both promoters were cloned as transcriptional *lux* reporters.

285 Based on the model of the *P. aeruginosa* AtuR repressor (37), a homolog of the
286 TetR repressor, we predicted that the *Pseudomonas* *sp.* OST1909 AtuR homolog binds
287 to and therefore senses acyclic naphthenic acid compounds, which relieves this repressor
288 from its inverted repeat binding site, resulting in induction of the *atuA-F* cluster in the
289 presence of naphthenic acids. In *Pseudomonas* *sp.* OST1909, the *atu* cluster is induced
290 by acyclic naphthenic acids, which are likely degraded by these genes, which are similar
291 in structure to acyclic terpenes (**Fig 2B**).



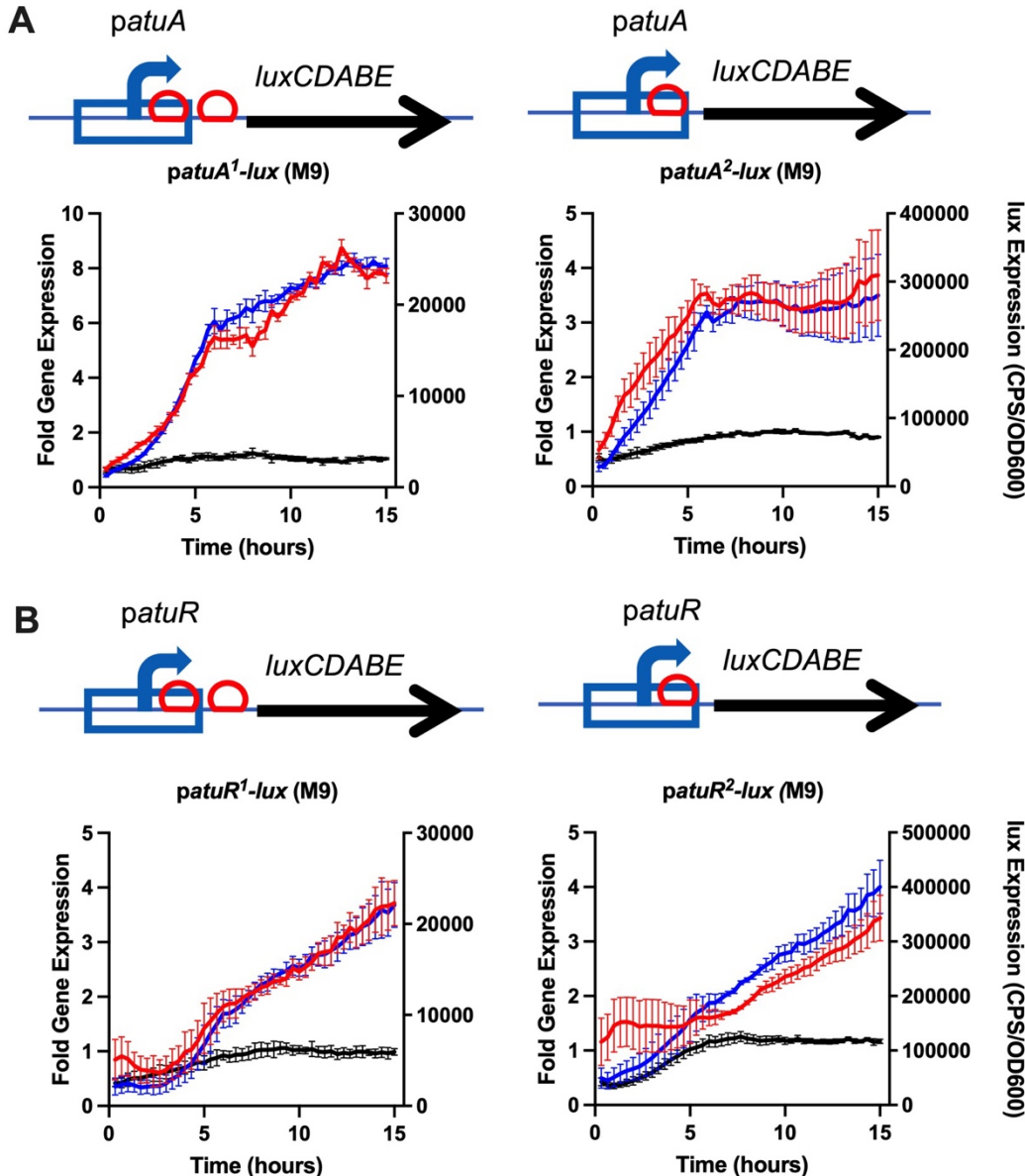
292

293 **Figure 2. Gene and promoter map of the *Pseudomonas* sp. OST1909 atu operon. A.**
294 Arrow diagrams demonstrate the order and orientation of the atu genes within the operon.
295 Sigma70-like promoters were found in the forward and reverse strand of the intergenic
296 region between atuR and atuA, shown as curved arrows. **B.** Chemical structure of
297 citronellol (acyclic terpene) and citronellate, which is a branched, acyclic naphthenic acid
298 (or terpene). **C.** Predicted, overlapping sigma-70 promoters with -10 and -35 regions.
299 AtuR dimers likely bind to inverted repeats (shown in grey) and represses expression of
300 both divergent promoters.

301

302 As shown in **Figure 3**, both first and second generation patuA-based biosensors
303 display a strong bioluminescent response to the acyclic NA mixture in defined M9 media.
304 For this comparison experiment, we used relatively high naphthenic acid concentrations
305 of 400 mg/L. In contrast to the complex NA mixtures extracted from OSPW, this
306 commercially available naphthenic acid extract is from a poorly defined petroleum source,
307 and mass spectrometry analyses of this sample demonstrated that most compounds are
308 acyclic naphthenic acids and range in length from 5-20 carbons (38, 18). Expression of
309 most biosensors was compared in BM2 and M9, both of which are similar defined growth

310 media, and overall, the base level expression and the naphthenic acid induction
311 responses were generally higher in M9 (data not shown). While the *atuA* expression
312 levels are generally lower in the first-generation biosensors, the peak fold gene
313 expression in the first-generation *patuA¹-lux* biosensor is higher (~8 fold) than that of the
314 second-generation sensor (~3.5 fold) (**Fig 3A**). In general, we interpret the biosensors
315 with highest induction response (peak fold change) as the most sensitive strains in
316 response to the analytes tested. The lower gene expression of the first-generation
317 biosensor may be attributed to the extra 31 bp of DNA and the second RBS found within,
318 which may interfere with the translation of the *lux* operon.



319

320 **Figure 3. Gene expression response of first and second generation *atuA* and *atuR*-**

321 **based biosensors to the acyclic NA mix.** A) First and second generation *patuA*-*lux*

322 biosensors and B) first and second generation *patuR*-*lux* biosensors were cultured in M9

323 medium with 400 mg/L acyclic mix and *lux* expression (CPS/OD₆₀₀) over time was

324 compared to untreated controls, shown in blue and black, respectively. The fold induction

325 (shown in red) is calculated by dividing the expression in the presence of NA by the control

326 media. All values shown are the average and standard deviation of triplicates, and each

327 experiment was performed 3 times.

328

329 **The *atuR* promoter is also induced in response acyclic naphthenic acids.** The
330 divergent *atuA* and *atuR* promoters are predicted to be regulated by AtuR, a
331 transcriptional repressor from the TetR family of regulators (39, 40) (**Fig 2**). Binding to the
332 inverted repeat operator by AtuR would repress both promoters, and both promoters are
333 predicted to be induced by naphthenic acid binding to AtuR. The *atuR* promoter was also
334 cloned as first and second-generation biosensors. While the second generation *patuR²*-
335 *lux* had roughly a 10X fold higher levels of overall expression, there was very little
336 difference in the maximum fold gene expression (4-fold) between the two biosensor
337 designs, which might be due to the slower induction response of this promoter compared
338 to *patuA* (**Fig 3B**). The *patuR*-based biosensor construct reaches a maximum fold
339 induction after 15 hours, compared to the maximum response time of around 5-7 hours
340 for the *patuA*-based construct (**Fig 3**). In conclusion, the *atuA* promoter responds faster
341 and to higher fold changes to acyclic naphthenic acids, compared to the *atuR* promoter,
342 and is therefore a better choice as for biosensors that detect acyclic naphthenic acids. It
343 should be noted that gene expression responses to naphthenic acids begin within
344 minutes, although the maximal responses are within hours, indicating a very fast sensing
345 bacterial response (**Fig 3**).

346

347 **The *atuA* promoter responds specifically to acyclic naphthenic acids and not to**
348 **related hydrocarbons.** To test the range of specificity, the *atuA-L* biosensor construct
349 (see methods for details) was screened with decreasing concentrations of four different
350 NA mixtures, as well as 28 different individual hydrocarbon compounds at a concentration
351 of 50 mg/L. **Figure 4** indicates the specificity of the *atuA-L* biosensor is primarily to acyclic

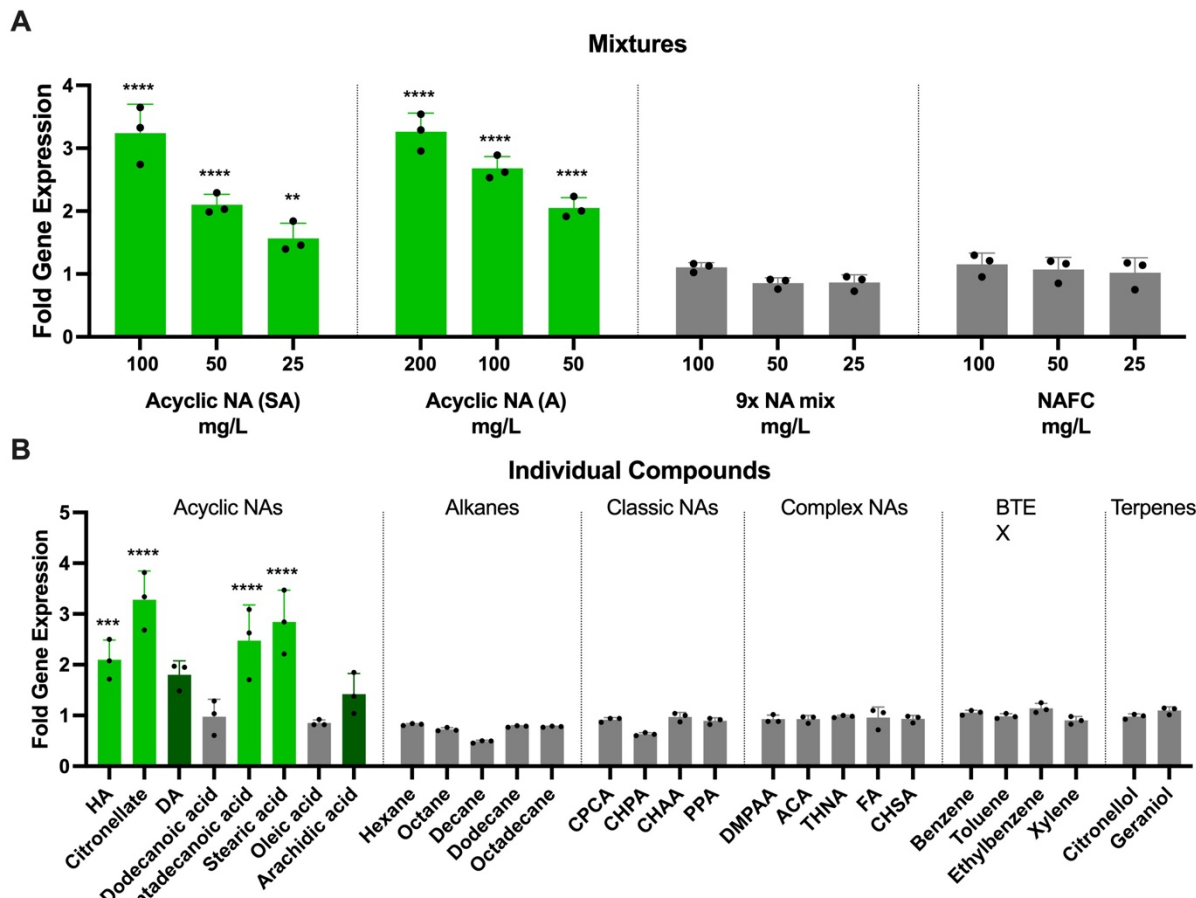
352 naphthenic acids. When exposed to diverse NA mixtures, the *atuA-L* construct displays
353 significant 2-fold *lux* expression patterns for both the commercially available acyclic NA
354 mixtures (18) (Sigma-Aldrich, Acros) at 50 mg/L (**Fig 4A**). The individual compounds
355 inducing the highest *lux* response from *atuA-L* are the acyclic NA compounds with low
356 and medium length carbon chains such as hexanoic acid (2-fold), citronellate (3-fold),
357 pentadecanoic acid (2.5-fold), and stearic acid (~2.8-fold) (**Fig 4B**). The *atuA* promoter
358 does not respond to any other related compounds, including ringed naphthenic acids,
359 alkanes or BTEX (benzene, toluene, ethylbenzene, xylene). Although the *atu* operon is
360 annotated in *P. aeruginosa* for the utilization of acyclic terpenes (citronellol) and
361 citronellate (16), the *atuA-L* biosensor responds to citronellate but does not exhibit a
362 bioluminescent response to terpenes like citronellol or geraniol (**Fig 4B**). This suggests
363 that the oil sands bacterial isolate *Pseudomonas sp.* OST1909 uniquely induces the *atu*
364 operon in response to acyclic naphthenic acids, rather than acyclic terpenes.

365

366

367

368



369

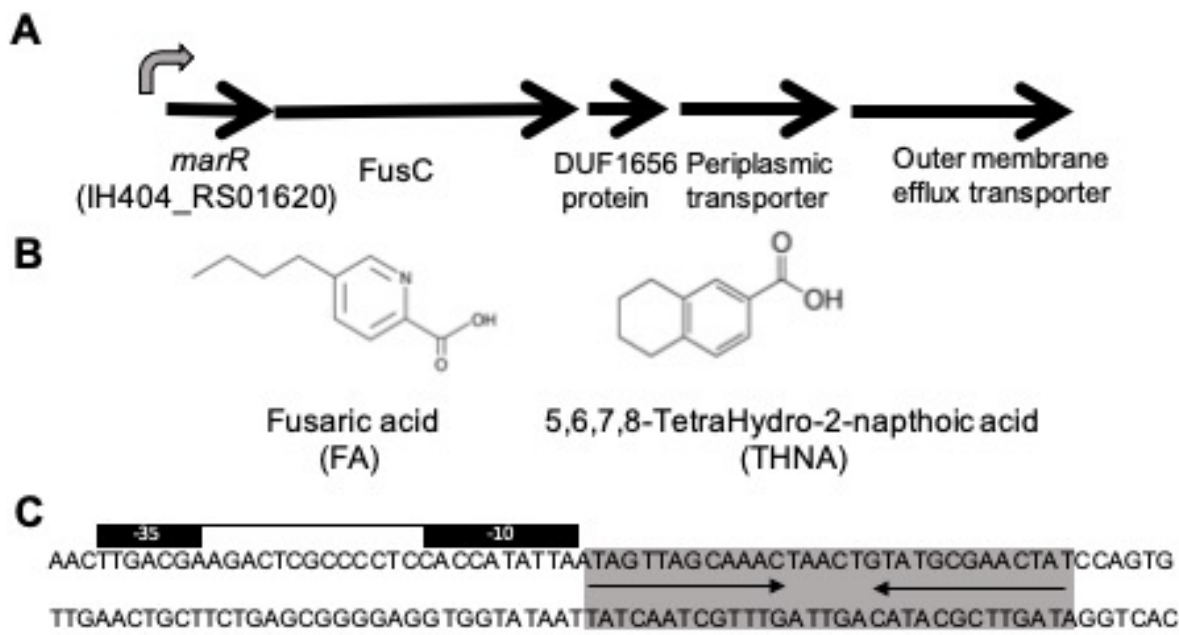
370 **Figure 4. Specificity of the atuA-L biosensor to naphthenic acid mixtures and**
371 **individual compounds. A.** The atuA-L biosensor was exposed to four different
372 naphthenic acid mixes with decreasing concentrations to monitor Fold gene expression
373 values. All values represent the average and standard deviation of triplicate values taken
374 at 6.6 hr. Sigma-Aldrich (SA) and Acros (A) indicate two commercial sources of acyclic
375 NA mixtures. A two-way ANOVA found that there was a statistically significant difference
376 between the mixtures ($F(3,32) = 134.6$, $p < 0.0001$) and concentrations ($F(3,32) = 81.12$,
377 $p < 0.0001$). **B.** Fold gene expression values of 28 different hydrocarbons at a
378 concentration of 50 mg/L. All values represent the average and standard deviation of
379 triplicate values taken at 3.3 hours. A one-way ANOVA revealed a statistically significant
380 difference between treatment groups ($F(28,58) = 20.96$, $p < 0.0001$). A post hoc Tukey
381 HSD test was then conducted with each compound and mix to test significant
382 relationships between each group ($\alpha = 0.05$, $n = 3$). Treatment groups with significant
383 results compared to the control are indicated with asterisks and bright green (*** indicate
384 $p < 0.001$, **** indicate $p < 0.0001$). Nonsignificant groups displaying fold gene expression
385 values above 1.5 are shown in dark green.

386

387

388 **The promoter regulating *marR* and antimicrobial resistance genes responds to**
389 **fusaric acid, an antibiotic with a naphthenic acid structure.** Among the genes
390 identified from the transcriptome study, an operon containing a MarR family regulator (41)
391 and genes predicted to contribute to fusaric acid transport, efflux and resistance (**Fig 5**),
392 was found to be upregulated in the transcriptome study by the acyclic NA mixture
393 (p<0.05, **Table 1, S3**). Fusaric acid is an antibiotic with a naphthenic acid structure that
394 has an aromatic ring containing a nitrogen heteroatom and two hydrocarbon branches
395 (**Fig 5B**).

396



397

398

399 **Figure 5. Gene map and promoter of the *marR* and naphthenic acid resistance**
400 **operon.** **A.** Arrow diagrams demonstrate the order and orientation of the genes encoding
401 a MarR family transcriptional regulator, FusC fusaric acid resistance transporter protein,
402 and an RND efflux pump. **B.** Fusaric acid has a naphthenic acid-like chemical structure,
403 and THNA is another complex naphthenic acid that induces *marR* expression **C.** The

404 sigma70-like promoter is located upstream of *marR*, indicated by the -10 and -35 regions,
405 which would be repressed by MarR binding to the predicted inverted repeat binding site
406 downstream of the promoter.

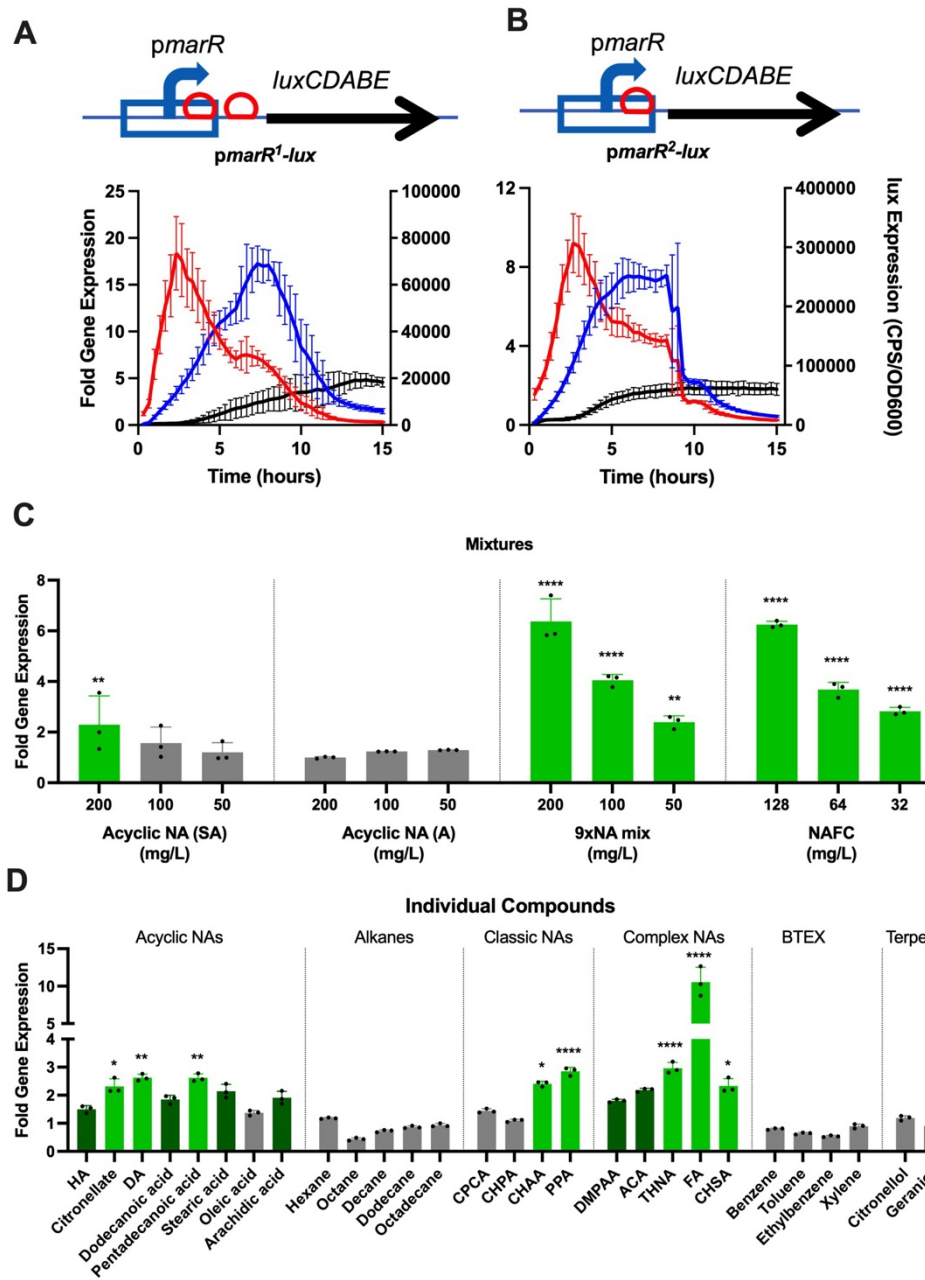
407

408 The *marR* gene found in *Pseudomonas* sp. OST1909 encodes a regulator
409 protein that is part of a large and widely distributed family of multiple antibiotic resistance
410 regulators (MarR) (41). This family of transcription factors is conceptually similar to the
411 TetR family, controlling many other cellular processes such as antibiotic resistance,
412 stress response (42), virulence (43), and degradation or export of harmful compounds
413 (44). Using the promoter region found upstream of the *marR* operon, first and second
414 generation *pmarR-lux* biosensors were constructed and tested for their responses to
415 multiple naphthenic acid mixtures. We demonstrated that both *pmarR*-based biosensor
416 constructs were strongly induced by fusaric acid, an antimicrobial with an NA-like
417 compound with a nitrogen-containing ring structure (**Fig 5B**). Similar to the *patuA*-based
418 biosensors, the first generation *marR* sensor has lower overall expression than the
419 second generation biosensor, but higher induction responses to fusaric acid, therefore
420 greater sensitivity (**Fig 6**). Gene expression reached a maximum within 3 hours and
421 rapidly decreased thereafter, which may represent a pattern of negative autoregulation.

422

423

424



425

426 **Figure 6. Detection of fusaric acid by first and second generation *pmarR*-based**
427 **biosensors and specificity of naphthenic acid detection.** Gene maps of **A)** first and
428 **B)** second generation *pmarR* biosensor are shown above their respective gene
429 expression *lux* response. Biosensors were exposed to 25 mg/L fusaric acid and *lux*
430 expression over time was compared to untreated media controls, shown in blue and
431 black, respectively. Fold gene expression values are shown in red. Values shown are the
432 average and standard deviation of triplicates, and each experiment was performed at
433 least 3 times. **C)** Fold gene expression values from the *marR-L* biosensor of four different
434 naphthenic acid mixes tested across a range of concentrations. SA (Sigma-Aldrich) and
435 NAFC

436 extracts. A two-way ANOVA found that there was a statistically significant difference
437 between the mixtures ($F(4,40) = 71.49$, $p < 0.0001$) and concentrations ($F(3,40) = 91.68$,
438 $p < 0.0001$). **D)** Fold gene expression values of 28 different hydrocarbons at a
439 concentration of 50 mg/L. A one-way ANOVA revealed a statistically significant difference
440 between treatment groups ($F(28,58) = 66.35$, $p < 0.0001$). A post hoc Tukey HSD test
441 was then conducted with each compound and mix to test significant relationships between
442 each group ($\alpha = 0.05$, $n = 3$). Treatment groups with significant results compared to the
443 control are indicated with asterisks and bright green (* indicate p values below 0.05, **
444 indicate p values below 0.01, **** indicate p values below 0.0001). Nonsignificant groups
445 displaying fold gene expression values above 1.5 are shown in dark green. All fold change
446 values shown represent the average of triplicates +/- standard deviation after 3 hours of
447 exposure and each experiment was performed 3 times.

448

449

450 **Specificity of naphthenic acid detection by the *marR* promoter.** To identify the range
451 of naphthenic acids compounds detected, the *marR*-L biosensor was screened with
452 decreasing concentrations of four different NA mixtures, as well as 28 different individual
453 compounds at a concentration of 50 mg/L. The *marR* promoter showed a modest
454 induction response to high concentrations of the Sigma-Aldrich acyclic NA mixtures (**Fig**
455 **6C**), which was consistent with the RNA-seq data ($p < 0.05$, **Table 1**). However, the *marR*
456 promoter was induced in a dose-dependent manner to a custom mix of 9 individual NA
457 compounds (50-200 mg/L), as well as extracted NA from oilsands process-affected water
458 (OSPW) (32-128 mg/L) (**Fig 6C**). As fusaric acid resistance genes are induced in the
459 presence of fusaric acid (45, 46), and in response to NAFC, this suggests the presence
460 of antimicrobial NA compounds, or FA, within the complex NAFC mixture.

461 When tested for the detection of individual compounds, the *marR* promoter was
462 specifically induced by a few acyclic NA structures, but mostly by complex and classic NA
463 structures. The strongest inducing compound was fusaric acid (FA, 10-fold), followed by
464 5,6,7,8-tetrahydro-2-naphthoic acid (THNA, 3-fold), 3-phenylpropionic acid (PPA, 3-fold),

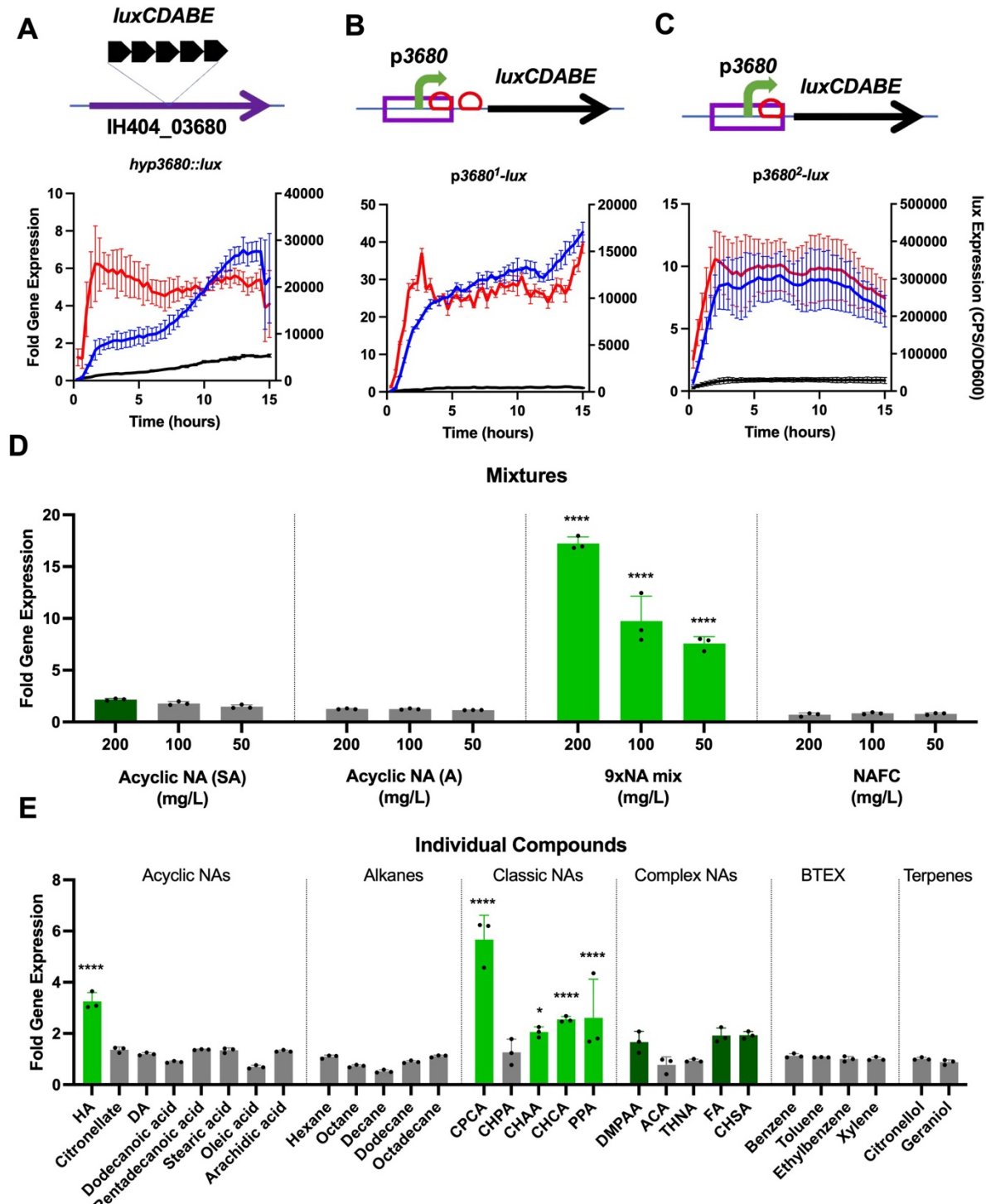
465 cyclohexyl succinic acid (CHSA, 2.5-fold), and cyclohexane acetic acid (CHAA, 2.5-fold)
466 (**Fig 6D**). The inducing acyclic NA included the branched compound citronellate, and
467 longer chain compounds such as decanoic acid and pentadecanoic acid (**Fig 6D**). In
468 summary, the *marR*-based biosensor detected diverse and complex NA mixtures and
469 compounds and was the only sensor to strongly respond to naphthenic acids extracted
470 from the OSPW from oil sands mining tailings ponds.

471

472 **A hypothetical gene promoter for detecting simple naphthenic acids.** The promoter
473 for a hypothetical gene at the locus tag IH404_RS03680 (referred to subsequently as
474 '3680'), was upregulated in the presence of the custom NA mixture from the RNA-seq
475 analysis (**Table S3**). While there are few identifiable functional domains in the 3680
476 protein, it does have three n-myristoylation sites, indicating post-translational modification
477 with the 14-carbon unsaturated fatty acid, myristic acid. Further evidence of a potential
478 role in fatty acid biology is suggested by the adjacent TetR regulator, a homolog of
479 *Pseudomonas aeruginosa* DesT that detects the ratios of unsaturated to saturated fatty
480 acids and regulates the production of unsaturated fatty acids for membrane lipid synthesis
481 (47). We also identified a mini-Tn5-*lux* insertion mutant within this gene (*hyp3680::lux*),
482 that also was strongly induced in the presence of the simple NA mixture (**Fig 7A**).

483 Based on the gene expression responses and a potential role in fatty acid biology,
484 this promoter was prioritized for synthesis and construction as a plasmid based p3680-
485 *lux* biosensor candidate. The chromosomal and plasmid-based p3680-based biosensors
486 were all strongly induced during growth in the presence of 50 mg/L of the simple 9xNA
487 mix (**Fig 7A-C**). The second-generation 3680 sensor exhibited almost 10-times the *lux*

488 expression of all constructs (**Fig 7BC**), consistent with the *atuA*, *atuR* and *marR*
489 expression patterns (**Figs 3, 6**). However, the first-generation *p3680¹-lux* sensor
490 displayed the highest fold gene expression values (**Fig 7B**) and was therefore the most
491 sensitive to NA detection.



492

493

494

495 **Figure 7. Detection of the simple 9x NA mixture with p3680-based biosensors and**
496 **specificity to individual naphthenic acid compounds.** Gene expression response
497 from **A)** chromosomal *hyp3680::lux* reporter **B)** first generation *p3680¹-lux* biosensor **C)**
498 second generation *p3680²-lux* biosensor after exposure to 50 mg/L of the simple 9xNA
499 mix (blue) and compared to untreated media controls (black). Fold gene expression
500 values are shown in orange. Gene maps for each biosensor are shown above their
501 respective *lux* response. All values shown are the average and standard deviation of
502 triplicates and each experiment was performed at least 3 times. **D)** Fold gene expression
503 values of four different naphthenic acid mixes with decreasing concentrations. SA (Sigma-
504 Aldrich) and A (Acros) indicate two sources of acyclic NA mixtures. A two-way ANOVA
505 found that there was a statistically significant difference between the mixtures ($F(3,32) =$
506 427.9, $p < 0.0001$) and concentrations ($F(3,32) = 92.50$, $p < 0.0001$). **E)** Fold gene
507 expression values of 28 different hydrocarbons at a concentration of 50 mg/L. A one-way
508 ANOVA revealed a statistically significant difference between treatment groups ($F(28,58)$
509 = 21.66, $p < 0.0001$). A post hoc Tukey HSD test was then conducted with each
510 compound and mix to test significant relationships between each group ($\alpha = 0.05$, $n = 3$).
511 Treatment groups with significant results compared to the control are indicated with
512 asterisks and bright green (** indicate p values below 0.001, **** indicate p values below
513 0.0001). Nonsignificant groups displaying fold gene expression values above 2 are shown
514 in dark green. All fold change values shown represent the average of triplicates +/-
515 standard deviation and each experiment was performed 3 times.

516

517 **Specificity of naphthenic acid detection by the hypothetical 3680 promoter.** The
518 *p3680²-lux* biosensor responded in a dose-dependent manner primarily to the custom
519 mixture of 9xNA compounds, but not to OSPW extracts or acyclic NA (**Fig 7D**). After
520 testing each separate compound from the 9xNA Mix, the *p3680²-lux* biosensor responded
521 mainly to the “classic” NA, such as cyclopentane carboxylic acid (CPCA, 6-fold),
522 cyclohexane carboxylic acid (CHCA, 3 fold), phenylpropionic acid (PPA, 3-fold) and
523 cyclohexane hexanoic acid (CHAA, 2 fold). Additionally, a significant 3-fold *lux* response
524 was seen with hexanoic acid (HA, 3-fold), a short acyclic NA that is also present in the
525 custom mixture (**Fig 7E**). This sensor also responds weakly (~ 2-fold) to other more
526 complex NA compounds such as 4-dimethylphenylacetic acid (DMPAA) and two
527 compounds absent from the mix, cyclohexane succinic acid (CHSA) and FA.

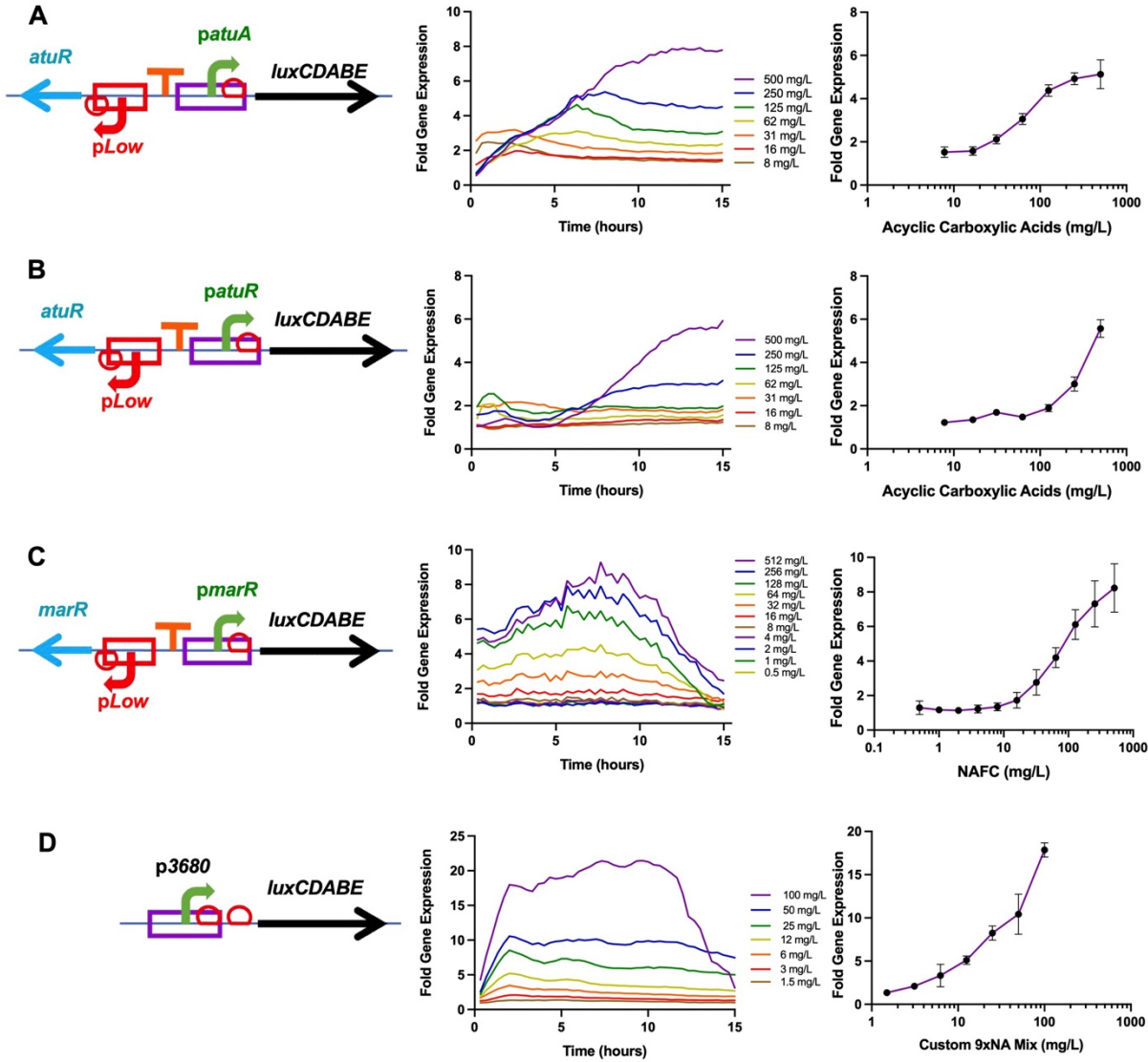
528

529 **Dose response assays and limits of detection of the *atuA*, *atuR*, *marR* and 3680**

530 **promoters.** The third-generation biosensor constructs were used to determine the
531 sensitivity and specificity of the *atuA*, *atuR* and *marR* promoters. These complete
532 biosensor constructs consist of the NA-inducible promoter fused to the *lux* reporter, with
533 the inclusion of the corresponding repressor protein, under control of a “Low” strength,
534 constitutive promoter. The *atuA*-L construct exhibits a linear relationship between the fold
535 expression change values ranging from 7.8 – 125 mg/L, while the *atuR*-L construct
536 displays this linear range of NA response and detection between 62.5 – 500 mg/L. The
537 *atuR* promoter responds more slowly, with lower fold changes and less sensitivity to
538 acyclic NA mixtures (**Fig 8 A,B**). The limit of sensitivity for these promoters was
539 determined by the NA concentration that resulted in a ~2-fold gene induction (biologically
540 relevant) and where increasing the concentration also increased the gene expression.
541 The limits of sensitivity were estimated to be 15 mg/L for the *atuA* promoter, and 125 mg/L
542 for the *atuR* promoter, in response to acyclic NA.

543

544



545

546 **Figure 8. Dose responses and sensitivity of the atuA-L, atuR-L, marR-L and p3680²-
547 lux biosensors to various NA mixtures.** Gene maps of each biosensor are displayed
548 on the left, gene expression in varying NA concentrations is shown in the middle, and
549 dose-response curves are on the right. **A)** Fold gene expression values of atuA-L were
550 calculated after exposure to increasing concentrations of acyclic NA, from 8 mg/L to 500
551 mg/L. **B)** Fold gene expression values of atuR-L were calculated after exposure to
552 increasing concentrations of acyclic NA, from 8 mg/L to 500 mg/L. **C)** Fold gene
553 expression values of marR-L were calculated after exposure to increasing concentrations
554 of NAFC, from 0.5 mg/L to 512 mg/L. **D)** Fold gene expression values of p3680²-lux were
555 calculated after exposure to increasing concentrations of the simple, 9xNA mix. All values
556 shown are the average of triplicate experiments +/- the standard deviation, and each
557 experiment was performed 3 times.

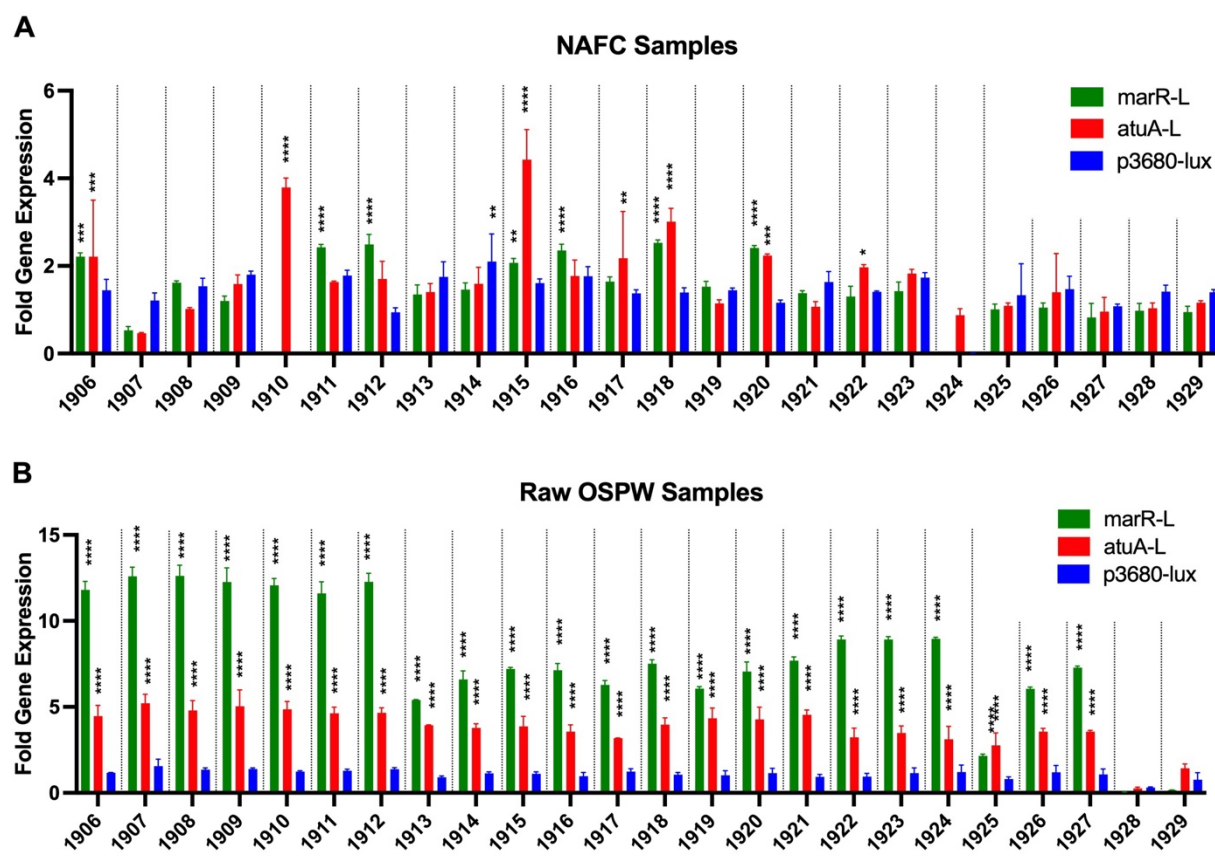
558

559 The third generation marR-L construct (*pLow-MarR*, *pmarR²-lux*) was screened
560 against 12 concentrations of the OSPW mixture ranging from 0.5 to 512 mg/L and the
561 resulting bioluminescence measurements are shown in **Figure 8C**. The *marR* promoter
562 responded to NAFC at concentrations as low as 16 mg/L, then responded in a linear dose
563 response as the concentration increased to 512 mg/L. The second generation *p3680²-lux*
564 biosensor construct was screened with 8 concentrations of the 9xNA mixture, ranging
565 from 1.5 - 100 mg/L (**Fig 8D**). This promoter responds very rapidly to the custom NA
566 mixture and exhibits a strong linear, dose-dependent bioluminescent response, where the
567 limit of detection of this custom 9XNA mix was as low 1.5 mg/L. (**Fig 8D**).
568

569 **Detection of naphthenic acids in OSPW samples using a panel of three NA-**
570 **inducible promoters.** In addition to demonstrating biosensor detection of individual NA
571 compounds and concentrated mixtures, it is important to also determine the ability of
572 these whole-cell biosensors to detect naphthenic acids in actual samples of oil sands
573 process-affected water (OSPW). We tested the NA biosensors for their ability to detect
574 naphthenic acids in a panel of 24 oil sands process-affected water samples, as well as
575 NAFC that were extracted from each respective OSPW sample. Given the wide range of
576 NAFC concentrations within the OSPW extracts (**Table S1**), we diluted these samples by
577 a factor of 10 or 100 in order to test a final NA concentration between 20 and 60 mg/L. In
578 **Figure 9A**, 11/24 NAFC extracts induced a significant biosensor response above
579 background expression levels (> 1-fold), from at least one of three whole cell biosensors.
580 Each biosensor in this collection responds to specific NA compounds (**Figs 4-8**), which
581 allows the estimation of abundant NA compounds present within these OSPW samples.

582 For example, samples 1911, 1912, and 1916 resulted in a ~2.5-fold *lux* response from
583 marR-L, suggested that more complex multi-ringed or phenolic compounds are abundant
584 in these mixtures. The *lux* response of atuA-L to the samples 1910 (~3.5-fold), 1917 (~2-
585 fold), and 1922 (~2-fold), suggested that these samples have a significant proportion of
586 acyclic NA compounds. NAFC extracted from OSPW are complex, and not surprisingly,
587 samples 1906, 1915, 1918, and 1920 induced a bioluminescent response multiple
588 sensors, indicating the presence complex and acyclic NA. The average 2-3-fold *lux*
589 response of both atuA-L and marR-L to the NAFC extracts screened at ~40 mg/L in
590 **Figure 9A** is similar to what would be expected from the standard curves (**Fig 8**).

591



592

593 **Figure 9. Specificity of marR-L, atuA-L, and *p3680²-lux* to NAFC extracts and raw**

594 **OSPW samples.** Fold gene expression values of marR-L, atuA-L, and the second

595 generation *p3680²-lux* biosensor were taken at 8 hours, 7 hours, and 3 hours,

596 respectively. **A.** Biosensor response to ~40 mg/L of each sample of NAFC extracts from

597 the OSPW. A two-way ANOVA found a statistically significant difference between

598 biosensor strains ($F(2,150) = 27.85$, $p < 0.0001$) and NAFC samples ($F(24,150) = 25.41$,

599 $p < 0.0001$). **B.** Biosensor response to the oil sands process-affected water samples. A

600 two-way ANOVA found a statistically significant difference between biosensor strains

601 ($F(2,150) = 5867$, $p < 0.0001$) and raw OSPW samples ($F(24,150) = 194.0$, $p < 0.0001$).

602 A post hoc Tukey HSD test was then conducted with each water sample and extract to

603 test significant relationships between each group ($\alpha = 0.05$, $n = 3$). Treatment groups with

604 significant results compared to the control are indicated with asterisks (* $p < 0.05$, ** $p <$

605 0.01, *** $p < 0.001$, **** $p < 0.0001$).

606

607 Due to the low NA concentrations reported for the water samples (**Table S1**), 90

608 μ l of each water sample were added to each well of the assay plate, with the addition 10

609 μ l of 10x BM2 growth media, to allow for minimal dilution of the OSPW sample. In **Figure**

610 **9B**, the biosensor panel performed much better, where 22/24 water samples induced a

611 significant biosensor response, from at least two of three whole cell biosensors. The

612 marR-L and atuA-L biosensors displayed a high fold expression response (between 4

613 and 12-fold) for all samples except two, while the promoter for 3680 did not respond to

614 any water sample. The discrepancy between the biosensor outputs when exposed to a

615 water samples and extracts of the same water sample could possibly be explained by a

616 bias or inefficiency in NA extraction of tailings water samples.

617

618 **Conclusions**

619 Whole cell bacterial biosensors have been previously constructed that are specific

620 to various hydrocarbons, including alkanes (48, 49), benzene/BTEX (50, 51) and

621 naphthalene (52). Here we describe a bacterial biosensor approach to construct

622 naphthenic acid biosensors. We identified several strong inducible promoters capable of
623 NA sensing, driving the expression of genes involved in degradation or protection from
624 NA. A transcriptome approach was used for the discovery of NA-induced genes, although
625 there were relatively few significantly induced genes when exposed to various NA
626 extracts, compared to other genomic studies (53). This may have been a limitation of
627 using duplicates for the transcriptome studies, but the use of transcriptional *lux* fusions
628 validated many of the upregulated genes identified by RNA-seq. Many fatty acid
629 degradation genes that likely contribute to β -oxidation of naphthenic acids were identified,
630 which is consistent with the results of a proteomic study with *Pseudomonas fluorescens*
631 Pf-5 (53). This study identified transcriptional repressors that may act as naphthenic acid
632 sensing proteins. The TetR and MarR family of transcription factors are well characterized
633 to sense and respond to small molecules, and in turn regulating a wide variety of cellular
634 processes including multidrug efflux pumps and carbon utilization. For these reasons,
635 small molecule sensing repressor proteins are commonly used in the construction of
636 bacterial biosensors (11, 48, 54).

637

638 The NA biosensors in this study can sense and respond to different NA mixtures
639 with good sensitivity, and each promoter demonstrates a unique naphthenic acid
640 specificity profile. The NA-induced promoters are strongly induced in a concentration-
641 dependent manner, which may allow for estimation of NA concentrations in OSPW by
642 extrapolation from the standard curve of gene expression responses (**Fig 8**). When used
643 to detect NA in small volume samples of water taken from tailings ponds, there was NA
644 detection by 2/3 biosensors in almost all water samples. When NAFC of those

645 corresponding water samples were tested at ~40 mg/L, fewer samples were detected,
646 which may be due to a change in NA composition after organic extraction. The ability to
647 test small volumes of raw water samples provides another advantage of minimal sample
648 preparation. Naphthenic acid biosensors show great potential for a rapid, reliable, cost-
649 effective, and semi-quantitative method for detection of environmental pollutants.

650

651 **Acknowledgements.** The authors acknowledge Laetitia Mazenod and Rich Moore for
652 technical assistance, and Paul Gordon for bioinformatics support. Funding was provided
653 by an NSERC Discovery Grant and Mitacs Canada.

654 **References**

655 1. Foght JM, Gieg LM, Siddique T. 2017. The microbiology of oil sands tailings: past,
656 present, future. *FEMS Microbiology Ecology* 93:fix034.

657 2. Kannel PR, Gan TY. 2012. Naphthenic acids degradation and toxicity mitigation in
658 tailings wastewater systems and aquatic environments: A review. *Journal of
659 Environmental Science and Health, Part A* 47:1–21.

660 3. Whitby C. 2010. Microbial Naphthenic Acid Degradation, p. 93–125. *In Advances in
661 Applied Microbiology*. Elsevier.

662 4. Vander Meulen IJ, Schock DM, Parrott JL, Mundy LJ, Pauli BD, Peru KM, McMartin
663 DW, Headley JV. 2021. Characterization of naphthenic acid fraction compounds in
664 water from Athabasca oil sands wetlands by Orbitrap high-resolution mass
665 spectrometry. *Sci Total Environ* 780:146342.

666 5. Li C, Fu L, Stafford J, Belosevic M, Gamal El-Din M. 2017. The toxicity of oil sands
667 process-affected water (OSPW): A critical review. *Science of The Total
668 Environment* 601–602:1785–1802.

669 6. Vander Meulen IJ, Klemish JL, Peru KM, Chen DDY, Pyle GG, Headley JV. 2021.
670 Molecular profiles of naphthenic acid fraction compounds from mine lease wetlands
671 in the Athabasca Oil Sands Region. *Chemosphere* 272:129892.

672 7. Huang R, Chen Y, Meshref MNA, Chelme-Ayala P, Dong S, Ibrahim MD, Wang C,
673 Klamerth N, Hughes SA, Headley JV, Peru KM, Brown C, Mahaffey A, Gamal El-
674 Din M. 2018. Characterization and determination of naphthenic acids species in oil

675 sands process-affected water and groundwater from oil sands development area of
676 Alberta, Canada. *Water Research* 128:129–137.

677 8. Clemente JS, Fedorak PM. 2005. A review of the occurrence, analyses, toxicity,
678 and biodegradation of naphthenic acids. *Chemosphere* 60:585–600.

679 9. Giesy JP, Anderson JC, Wiseman SB. 2010. Alberta oil sands development.
680 Proceedings of the National Academy of Sciences 107:951–952.

681 10. Hindle, R, Headley J, Muench, D.G. 2023. Pros and Cons of Separation,
682 Fractionation and Cleanup for Enhancement of the Quantitative Analysis of
683 Bitumen-Derived Organics in Process-Affected Waters—A Review. *Separations*
684 10:583.

685 11. van der Meer JR, Belkin S. 2010. Where microbiology meets microengineering:
686 design and applications of reporter bacteria. *Nat Rev Microbiol* 8:511–522.

687 12. Fernandez-López R, Ruiz R, de la Cruz F, Moncalián G. 2015. Transcription factor-
688 based biosensors enlightened by the analyte. *Frontiers in Microbiology* 6:648.

689 13. van der Meer JR, Belkin S. 2010. Where microbiology meets microengineering:
690 design and applications of reporter bacteria. *Nat Rev Microbiol* 8:511–522.

691 14. Zhang D, He Y, Wang Y, Wang H, Wu L, Aries E, Huang WE. 2012. Whole-cell
692 bacterial bioreporter for actively searching and sensing of alkanes and oil spills.
693 *Microb Biotechnol* 5:87–97.

694 15. Ray S, Panjikar S, Anand R. 2018. Design of Protein-Based Biosensors for
695 Selective Detection of Benzene Groups of Pollutants. *ACS Sens* 3:1632–1638.

696 16. Aleksic J, Bizzari F, Cai Y, Davidson B, Mora K de, Ivakhno S, Seshasayee SL,
697 Nicholson J, Wilson J, Elfick A, French C, Kozma-Bognar L, Ma H, Millar A. 2007.
698 Development of a novel biosensor for the detection of arsenic in drinking water. *IET
699 Synthetic Biology* 1:87–90.

700 17. Shideler S, Headley J, Gauthier J, Kukavica-Ibrulj I, Levesque RC, Lewenza S.
701 2021. Complete Genome Sequence of a *Pseudomonas* Species Isolated from
702 Tailings Pond Water in Alberta, Canada. *Microbiology Resource Announcements*
703 <https://doi.org/10.1128/MRA.01174-20>.

704 18. Marentette JR, Frank RA, Bartlett AJ, Gillis PL, Hewitt LM, Peru KM, Headley JV,
705 Brunswick P, Shang D, Parrott JL. 2015. Toxicity of naphthenic acid fraction
706 components extracted from fresh and aged oil sands process-affected waters, and
707 commercial naphthenic acid mixtures, to fathead minnow (*Pimephales promelas*)
708 embryos. *Aquat Toxicol* 164:108–117.

709 19. Headley, J.V., Peru, K.M., Fahlman, B., Colodey, A., McMartin, D.W. 2013.
710 Selective solvent extraction and characterization of the acid extractable fraction of
711 Athabasca oil sands process waters by Orbitrap mass spectrometry. *International
712 Journal of Mass Spectrometry* 345–347:104–108.

713 20. Rumble SM, Lacroix P, Dalca AV, Fiume M, Sidow A, Brudno M. 2009. SHRiMP:
714 accurate mapping of short color-space reads. *PLoS Comput Biol* 5:e1000386.

715 21. Bray NL, Pimentel H, Melsted P, Pachter L. 2016. Near-optimal probabilistic RNA-
716 seq quantification. *Nat Biotechnol* 34:525–527.

717 22. Pimentel H, Bray NL, Puente S, Melsted P, Pachter L. 2017. Differential analysis of
718 RNA-seq incorporating quantification uncertainty. *Nat Methods* 14:687–690.

719 23. Duan K, Dammel C, Stein J, Rabin H, Surette MG. 2003. Modulation of
720 *Pseudomonas aeruginosa* gene expression by host microflora through interspecies
721 communication. *Molecular Microbiology* 50:1477–1491.

722 24. Johns NI, Gomes ALC, Yim SS, Yang A, Blazejewski T, Smillie CS, Smith MB, Alm
723 EJ, Kosuri S, Wang HH. 2018. Metagenomic mining of regulatory elements
724 enables programmable species-selective gene expression. 5. *Nat Methods*
725 15:323–329.

726 25. Solovyev V, Salamov A. 2011. Automatic Annotation of Microbial Genomes and
727 Metagenomic Sequences., p. 61–78. *In* Li, RL (ed.), *Metagenomics and its*
728 *Applications in Agriculture, Biomedicine and Environmental Studies*. Nova Science
729 Publishers.

730 26. Chen Y-J, Liu P, Nielsen AAK, Brophy JAN, Clancy K, Peterson T, Voigt CA. 2013.
731 Characterization of 582 natural and synthetic terminators and quantification of their
732 design constraints. 7. *Nat Methods* 10:659–664.

733 27. Lewenza S, Falsafi RK, Winsor G, Gooderham WJ, McPhee JB, Brinkman FSL,
734 Hancock REW. 2005. Construction of a mini-Tn5-luxCDABE mutant library in

735 Pseudomonas aeruginosa PAO1: a tool for identifying differentially regulated
736 genes. *Genome Res* 15:583–589.

737 28. Wilton M, Halverson TWR, Charron-Mazenod L, Parkins MD, Lewenza S. 2018.
738 Secreted Phosphatase and Deoxyribonuclease Are Required by Pseudomonas
739 aeruginosa To Defend against Neutrophil Extracellular Traps. *Infect Immun*
740 86:e00403-18.

741 29. Jain PT, Pento JT. 1991. A vehicle for the evaluation of hydrophobic compounds in
742 cell culture. *Res Commun Chem Pathol Pharmacol* 74:105–116.

743 30. Hong Y-H, Deng M-C, Xu X-M, Wu C-F, Xiao X, Zhu Q, Sun X-X, Zhou Q-Z, Peng
744 J, Yuan J-P, Wang J-H. 2016. Characterization of the transcriptome of
745 Achromobacter sp. HZ01 with the outstanding hydrocarbon-degrading ability. *Gene*
746 584:185–194.

747 31. Fida TT, Moreno-Forero SK, Breugelmans P, Heipieper HJ, Röling WFM, Springael
748 D. 2017. Physiological and Transcriptome Response of the Polycyclic Aromatic
749 Hydrocarbon Degrading *Novosphingobium* sp. LH128 after Inoculation in Soil.
750 *Environ Sci Technol* 51:1570–1579.

751 32. Das D, Mawlong GT, Sarki YN, Singh AK, Chikkaputtaiah C, Boruah HPD. 2020.
752 Transcriptome analysis of crude oil degrading Pseudomonas aeruginosa strains for
753 identification of potential genes involved in crude oil degradation. *Gene*
754 755:144909.

755 33. Zarzycki-Siek J, Norris MH, Kang Y, Sun Z, Bluhm AP, McMillan IA, Hoang TT.
756 2013. Elucidating the *Pseudomonas aeruginosa* fatty acid degradation pathway:
757 identification of additional fatty acyl-CoA synthetase homologues. PLoS One
758 8:e64554.

759 34. Höschle B, Gnau V, Jendrossek D. 2005. Methylcrotonyl-CoA and geranyl-CoA
760 carboxylases are involved in leucine/isovalerate utilization (Liu) and acyclic terpene
761 utilization (Atu), and are encoded by liuB/liuD and atuC/atuF, in *Pseudomonas*
762 *aeruginosa*. Microbiology (Reading) 151:3649–3656.

763 35. Aguilar JA, Zavala AN, Díaz-Pérez C, Cervantes C, Díaz-Pérez AL, Campos-
764 García J. 2006. The atu and liu clusters are involved in the catabolic pathways for
765 acyclic monoterpenes and leucine in *Pseudomonas aeruginosa*. 3. Appl Environ
766 Microbiol 72:2070–2079.

767 36. Förster-Fromme K, Höschle B, Mack C, Bott M, Armbruster W, Jendrossek D.
768 2006. Identification of genes and proteins necessary for catabolism of acyclic
769 terpenes and leucine/isovalerate in *Pseudomonas aeruginosa*. 7. Appl Environ
770 Microbiol 72:4819–4828.

771 37. Förster-Fromme K, Jendrossek D. 2010. AtuR is a repressor of acyclic terpene
772 utilization (Atu) gene cluster expression and specifically binds to two 13 bp inverted
773 repeat sequences of the atuA-atuR intergenic region. FEMS Microbiol Lett
774 308:166–174.

775 38. Hao C, Headley JV, Peru KM, Frank R, Yang P, Solomon KR. 2005.
776 Characterization and pattern recognition of oil-sand naphthenic acids using
777 comprehensive two-dimensional gas chromatography/time-of-flight mass
778 spectrometry. *J Chromatogr A* 1067:277–284.

779 39. Ramos JL, Martínez-Bueno M, Molina-Henares AJ, Terán W, Watanabe K, Zhang
780 X, Gallegos MT, Brennan R, Tobes R. 2005. The TetR Family of Transcriptional
781 Repressors. *Microbiol Mol Biol Rev* 69:326–356.

782 40. Cuthbertson L, Nodwell JR. 2013. The TetR family of regulators. 3. *Microbiol Mol*
783 *Biol Rev* 77:440–475.

784 41. Deochand DK, Grove A. 2017. MarR family transcription factors: dynamic
785 variations on a common scaffold. *Critical Reviews in Biochemistry and Molecular*
786 *Biology* 52:595–613.

787 42. Atichartpongkul S, Vattanaviboon P, Wisitkamol R, Jaroensuk J, Mongkolsuk S,
788 Fuangthong M. 2016. Regulation of Organic Hydroperoxide Stress Response by
789 Two OhrR Homologs in *Pseudomonas aeruginosa*. *PLOS ONE* 11:e0161982.

790 43. Ellison DW, Miller VL. 2006. Regulation of virulence by members of the MarR/SlyA
791 family. *Curr Opin Microbiol* 9:153–159.

792 44. Sulavik MC, Gambino LF, Miller PF. 1995. The MarR repressor of the multiple
793 antibiotic resistance (mar) operon in *Escherichia coli*: prototypic member of a family
794 of bacterial regulatory proteins involved in sensing phenolic compounds. *Mol Med*
795 1:436–446.

796 45. Hu R-M, Liao S-T, Huang C-C, Huang Y-W, Yang T-C. 2012. An Inducible Fusaric
797 Acid Tripartite Efflux Pump Contributes to the Fusaric Acid Resistance in
798 *Stenotrophomonas maltophilia*. PLoS One 7:e51053.

799 46. Crutcher FK, Puckhaber LS, Stipanovic RD, Bell AA, Nichols RL, Lawrence KS, Liu
800 J. 2017. Microbial Resistance Mechanisms to the Antibiotic and Phytotoxin Fusaric
801 Acid. J Chem Ecol 43:996–1006.

802 47. Zhang Y-M, Zhu K, Frank MW, Rock CO. 2007. A *Pseudomonas aeruginosa*
803 transcription factor that senses fatty acid structure. Molecular Microbiology 66:622–
804 632.

805 48. Sticher P, Jaspers MC, Stemmler K, Harms H, Zehnder AJ, van der Meer JR.
806 1997. Development and characterization of a whole-cell bioluminescent sensor for
807 bioavailable middle-chain alkanes in contaminated groundwater samples. Appl
808 Environ Microbiol 63:4053–4060.

809 49. Reed B, Blazeck J, Alper H. 2012. Evolution of an alkane-inducible biosensor for
810 increased responsiveness to short-chain alkanes. J Biotechnol 158:75–79.

811 50. Applegate BM, Kehrmeyer SR, Sayler GS. 1998. A chromosomally based tod-
812 luxCDABE whole-cell reporter for benzene, toluene, ethybenzene, and xylene
813 (BTEX) sensing. Appl Environ Microbiol 64:2730–2735.

814 51. Kuncova G, Pazlarova J, Hlavata A, Ripp S, Sayler GS. 2011. Bioluminescent
815 bioreporter *Pseudomonas putida* TVA8 as a detector of water pollution.

816 Operational conditions and selectivity of free cells sensor., Ecological Indicators
817 11:882–887.

818 52. King JM, Digrizia PM, Applegate B, Burlage R, Sanseverino J, Dunbar P, Larimer
819 F, Sayler GS. 1990. Rapid, sensitive bioluminescent reporter technology for
820 naphthalene exposure and biodegradation. *Science* 249:778–781.

821 53. McKew BA, Johnson R, Clothier L, Skeels K, Ross MS, Metodiev M, Frenzel M,
822 Gieg LM, Martin JW, Hough MA, Whitby C. 2021. Differential protein expression
823 during growth on model and commercial mixtures of naphthenic acids in
824 *Pseudomonas fluorescens* Pf-5. *Microbiologyopen* 10:e1196.

825 54. Fernandez-López R, Ruiz R, de la Cruz F, Moncalián G. 2015. Transcription factor-
826 based biosensors enlightened by the analyte. *Front Microbiol* 6:648.

827

828

Table 1. *U* test analysis of upregulated operons from RNA-seq data.

Acyclic NA (SA)	p	q	log2fc (tpm)
AtuR	0.015	0.281	0.732
AtuA	0.000	0.000	1.383
AtuB	NA	NA	1.047
AtuC	0.000	0.000	1.663
AtuD	NA	NA	1.090
AtuE	NA	NA	0.673
AtuF	NA	NA	1.409

***U* test, p=0.01**

9xNA mix	p	q	log2fc (tpm)
MarR	0.000	0.031	1.473
MarA	0.000	0.000	1.418
MarB	NA	NA	1.279
MarC	0.000	0.043	0.892
MarD	0.000	0.007	1.312

***U* test, p=0.034**

Acyclic NA (SA)	p	q	log2fc (tpm)
MarR	0.002	0.083	1.217
MarA	0.000	0.000	1.334
MarB	NA	NA	1.192
MarC	0.000	0.000	1.183
MarD	0.081	0.613	0.548

***U* test, p=0.049**

829